A.V. NESTEROV, V.S. VASILEVSKY, T.P. KOVALENKO

Bogolyubov Institute for Theoretical Physics, Nat. Acad. of Sci. of Ukraine
(14b, Metrolohichna Str., Kyiv 03680, Ukraine; e-mail: nesterov@bitp.kiev.ua)

UDC 539

SPECTRA OF NUCLEI ^{9}Be AND ^{9}B IN A THREE-CLUSTER MICROSCOPIC MODEL

Within a microscopic three-cluster $\alpha+\alpha+$ n(p) model, which is a three-cluster version of the algebraic approach to the resonating group method (AV RGM), we consider the spectra of the low-lying states of mirror nuclei ^{9}Be and ^{9}B in the excitation energy range from zero to 5 MeV. The obtained theoretical results are compared with the available experimental data.

Keywords: spectra of nuclei, three-cluster microscopic model, resonating group method, energy range

1. Introduction

We will study the spectra of low-lying states of nuclei ^{9}Be and ^{9}B. As is known, nucleus ^{9}Be is bound only in the ground state, whereas nucleus ^{9}B, which is the mirror one relative to ^{9}Be, has no bound states at all. In other words, except for the ground state of nucleus ^{9}Be, we will deal mainly with resonance states, the interest in which is determined by a number of the following factors.

The study of the low-lying states of nucleus ^{9}Be is of interest for astrophysics, in particular, for the problem of nuclear synthesis of elements. The resonances lying above the threshold of disintegration of ^{9}Be determine the rate of synthesis of this nucleus under the bursts of supernovas. At sufficiently high concentrations of neutrons and alpha-particles in a star, the radiative capture reaction $\alpha(\alpha$n, $\gamma)^9$Be can run with high rate in the resonance mode. This reaction is followed by ^{9}Be $(\alpha$,n$)^{12}$C [1, 2]. Along with the three-alpha capture $\alpha(\alpha\alpha, \gamma)^{12}$C, the mentioned reactions can play a significant role in overcoming the barrier for the creation of elements with $A > 8$. This barrier is related to the absence of bound states of the nuclei with $A = 5$ and $A = 8$ (^{5}H, ^{5}Li, ^{8}Be), i.e., to the so-called "mass dip".

Of interest is also the comparison of the spectra of the low-lying states of mirror nuclei ^{9}Be and ^{9}B presenting the example of the influence of the Coulomb interaction of protons on the spectra of light atomic nuclei. Especially, this concerns the states $1/2^+$, $1/2^-$, and $5/2^+$. Despite the many-year efforts, there is no complete information about the energies and the widths of these resonances. In particular, the spins are known not for all states. Especially, this is true for ^{9}B. Moreover, its state $1/2^+$, which is analogous to that with an excitation energy of 1.68 MeV in nucleus ^{9}Be, was not given in the recent compiled work [3] among the detected experimentally states of nucleus ^{9}B.

The interest in the situation concerning these nuclei is manifested in a large number of experimental [4–11] and theoretical works [12–21] (we have indicated only a part of them) devoted to the consideration of properties of nuclei ^{9}Be and ^{9}B.

The choice of a model for the description of properties of the nuclei under consideration is determined by the domination of the three-cluster channels $\alpha+\alpha+$n and $\alpha+\alpha+$p at small energies. The threshold energies of these channels are minimal among all channels. We note that the next-in-energy threshold of the channel ^{7}Li+d in nucleus ^{9}Be (and ^{7}Be+d in ^{9}B), where the α-cluster is broken, is much higher than the threshold of the three-cluster channel (more than 15 MeV). Moreover, the α-clusters themselves have no excited states below approximately the same energy. Therefore, it is possible to assume surely that the low-energy spectrum of these nuclei is formed by the three-cluster channels $\alpha+\alpha+n$ and $\alpha+\alpha+p$, where the density distribution for nucleons in α-clusters can be considered frozen. This is also indicated by the energy position of the bound state of nucleus ^{9}Be: it is near the threshold of $\alpha+\alpha+n$, by 1.57 MeV below. It is worth noting that the three-cluster systems under consideration have no bound binary subsystems. In this case, the lifetimes of nuclei ^{8}Be and ^{5}He in

the ground state are, respectively, 0.97×10^{-16} and 1.1×10^{-21} s (4.4×10^{-22} s for ^{5}Li). This indicates that the cluster representation α+α+n (α+α+p) for nucleus ^{9}Be (^{9}B) dominates at comparatively low energies. This circumstance must be taken into account in a model for nuclei ^{9}Be and ^{9}B.

In the present work, we use the microscopic approach as such one, namely the three-cluster algebraic version of the resonating group method (see details in [22, 23]), where the function describing the relative motion of clusters is expanded in the eigenfunctions of a six-dimensional harmonic oscillator in hyperspherical coordinates.

The main positions of the model in use are briefly presented in Section 2, and the results are given in Section 3.

2. Method

The many-particle wave function of a three-cluster system consisting of A nucleons ($A = A_1 + A_2 + A_3$) with the full account for the antisymmetrization can be represented as

$$\Psi\left(q_1, .., q_{A-1}\right) = \hat{\mathcal{A}}\left[\Psi_1\left(A_1\right)\Psi_2\left(A_2\right)\Psi_3\left(A_3\right)\Psi_Q\left(Q\right)\right], \tag{1}$$

where $\hat{\mathcal{A}}$ is the operator of antisymmetrization. In this case, we assume that the center-of-mass coordinate for the A-nucleon system is excluded by the transition to the Jacobi coordinates q_i. This reduces the problem to the consideration of the internal dynamics of the system. The functions $\Psi_i\left(A_i\right)$ set the internal structure of the i-th cluster. The function

$$\Psi_Q\left(Q\right) = \Psi_Q\left(q_1, q_2\right) \tag{2}$$

characterizes the relative motion of clusters, depends on the Jacobi coordinates q_1 and q_2, and can be expanded in the approach under consideration in the basis of a six-dimensional harmonic oscillator.

Since the wave functions of clusters are fixed in our case and are constructed only on the $(0s)$-orbitals, the problem of classification of the states of the system after the expansion of the relative motion function in the basis is completely transferred onto the basis states describing the intercluster motion. In our specific case, such basis states are the eigenfunctions of a six-dimensional harmonic oscillator $|n_\rho, K, l_1, l_2, LM\rangle$. They are characterized by the hypermoment K, number of quanta of hyperradial excitations n_ρ, partial angular momenta l_1 and l_2 connected with the first and second Jacobi vectors, respectively, total angular momentum L produced by the coupling of the partial momenta l_1 and l_2, and its projection M. In this case, the relation $N = 2n_\rho + K$ holds for each oscillator shell with the principal quantum number N.

The expansion of the wave function of the relative motion

$$\Psi_Q\left(q_1, q_2\right) = \sum_\nu C_\nu \Psi_\nu\left(q_1, q_2\right), \tag{3}$$

where

$$\{\Psi_\nu\} = |n_\rho, K, l_1, l_2, LM\rangle (\nu = \{n_\rho, K, l_1 l_2, LM\}),$$

leads to the infinite system of algebraic equations

$$\sum_{\nu'} \left[\langle\nu|\hat{H}|\nu'\rangle - E\langle\nu|\nu'\rangle\right] C_{\nu'} = 0 \tag{4}$$

for the coefficients C_ν. Totally, these coefficients determine the wave function in the oscillator representation.

System (4) is a consequence of both the choice of a trial function in the form (1) and expansion (3), while solving the many-particle Schrödinger equation. The quantities $\langle\nu|\hat{H}|\nu'\rangle$ and $\langle\nu|\nu'\rangle$ are matrix elements of the Hamiltonian and the identity operator on the antisymmetrized many-particle basis functions $|\nu\rangle = |n_\rho, K, l_1, l_2, LM\rangle$. The presentation of the technique of calculations of these quantities required for the following consideration is omitted here for brevity (see works [22, 23] and references therein). We note only that, like the solution of the problems with a continuous or discrete spectrum, where the asymptotic formulas for the wave functions at large distances in the coordinate representation are used to set the boundary conditions, the solution in the oscillator representation involves a practically equivalent procedure. At large values of the number of radial oscillator quanta for the relative motion of clusters, we use again the asymptotic formulas, but already for the expansion coefficients C_ν.

In view of the results of works [24, 25], the expansion coefficients $C_{n_\rho}^{(\pm)}$ corresponding to incoming and outgoing waves can be presented at large values of the number of quanta of hyperradial excitations n_ρ as follows:

for uncharged clusters,

$$C_{n_\rho}^{(\pm)K} \simeq \sqrt{2} \begin{Bmatrix} H_{K+2}^{(1)}\left(k\rho_{n_\rho}\right) \\ H_{K+2}^{(2)}\left(k\rho_{n_\rho}\right) \end{Bmatrix}, \quad (5)$$

and, in the presence of the Coulomb interaction,

$$C_{n_\rho}^{(\pm)K} \simeq \sqrt{2} \begin{Bmatrix} W_{i\eta,K+2}\left(2ikb\rho_{n_\rho}\right)/\sqrt{\rho_{n_\rho}} \\ W_{-i\eta,K+2}\left(-2ikb\rho_{n_\rho}\right)/\sqrt{\rho_{n_\rho}} \end{Bmatrix}. \quad (6)$$

In formulas (5) and (6), $k = \sqrt{\frac{2mE}{\hbar^2}}$, the letters H and W stand for the Hankel and Whittaker functions, respectively, $\rho_{n_\rho} = b\sqrt{4n_\rho + 2K + 6}$, b is the oscillator radius, and η is the Sommerfeld parameter.

We note that the asymptotic solutions for neutral (uncharged) clusters depend exclusively only on the hypermoment K, rather than on all values of quantum numbers. In this case, the channels with different K are uncoupled. In this sense, it is logical to represent the compound index $\nu = \{n_\rho, K, (l_1 l_2) LM\}$ as $\nu = \{K, \nu_0\}$, by separating K among other quantum numbers. The asymptotic solutions for charged clusters depend on K and the partial angular momenta (see [29] for details). For short-range forces, the decoupling of channels at large values of n_ρ poses practically no problems. The case of Coulomb forces requires a somewhat higher attention, but we omit the discussion of related questions analyzed in works [22, 23]. Finally, we deal with the situation where the states with different K and ν_0 are connected by means of nuclear and Coulomb forces only in the internal domain (the interaction domain), i.e., we arrive at the approximation of coupled channels.

For the consideration of the asymptotics, it is convenient to write our system of equations in the form

$$\sum_{K', m_\rho} \left\langle n_\rho, K \left| \hat{H} - E \right| m_\rho, K' \right\rangle C_{m_\rho}^{K'} = 0, \quad (7)$$

where K stands for the collection of all indices except for n_ρ.

Since we will use the S-matrix formalism while solving the scattering problem, we represent the expansion coefficients $C_{n_\rho}^K$ at large values of n_ρ as

$$C_{n_\rho}^K = C_{n_\rho}^{(0)K} + \delta_{K_i K} C_{n_\rho}^{(-)K} - S_{K_i K} C_{n_\rho}^{(+)K}, \quad (8)$$

where, for each of the K-channels, $C_{n_\rho}^{(0)K}$ is the so-called residual coefficient, and $C_{n_\rho}^{(\pm)K}$ are asymptotic coefficients related to convergent and divergent waves. The matrix elements $S_{K_i K}$ describe the coupling between the output channel K and the input channel K_i.

The substitution of (8) in the equations of system (7) gives the system of dynamical equations for the multichannel problem. This system of equations will be solved in order to determine the residual coefficients $C_{n_\rho}^{(0)K}$ and the S-matrix elements $S_{K'K}$.

In order to optimally obtain the most exact approximation in the solution of the system, we will distinguish some internal domain with $n_\rho \leq N_\rho$ and the asymptotic domain with $n_\rho > N_\rho$. The choice of N_ρ should be such that the expansion coefficients $\left\{C_{n_\rho}^{(0)K}\right\}$ be characterized by the essential smallness in the asymptotic domain.

Solving the system of dynamical equations for each of N_{ch} input channels, we obtain the S-matrix $||S_{\nu,\nu'}||$, which contains a detailed information about the elastic and inelastic processes in the three-cluster system. It is convenient to analyze the S-matrix, by transforming it to the diagonal form. Such a representation of the S-matrix is usually called the representation of eigenchannels and leads to the so-called eigenphases of scattering δ_α:

$$S_\alpha = \exp\{2i\delta_\alpha\}, \quad \alpha = 1, 2, ..., N_{ch}, \quad (9)$$

where α enumerates the uncoupled eigenchannels.

The eigenphases of scattering are used to determine the parameters of resonances such as their energies and widths. With the help of the well-known formula for the r-th resonance in the α-eigenchannel, it is easy to find the energy and the width of the resonance:

$$\left.\frac{d^2\delta_\alpha}{dE^2}\right|_{E=E_{\alpha,r}} = 0, \quad \Gamma = 2\left(\frac{d\delta_\alpha}{dE}\right)^{-1}\Bigg|_{E=E_{\alpha,r}}. \quad (10)$$

3. Results

The results presented in this section are obtained with the Minnesota potential, whose central part is taken from work [26], and the spin-orbit one from work [27] (version IV). In calculations, the oscillator radius b was taken to be 1.285 Fm. This value of b minimizes the binding energy of each separate α-particle. The value of exchange parameter u in the potential is determined to be such that the binding energy for the ground state of nucleus ^{9}Be relative to the $\alpha + \alpha$+n threshold is reproduced. To attain the suitable accuracy of calculations, we used all hyperharmonics with

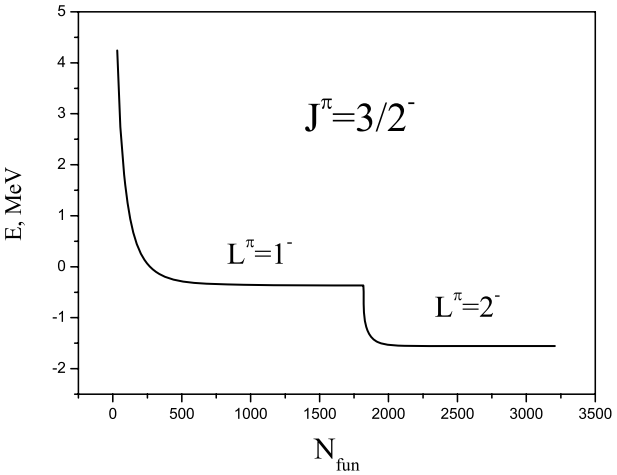

Fig. 1. Binding energy of the ground state of nucleus ^{9}Be versus the number of basis functions used in calculations

hypermoments $K \leq 13$ and $K \leq 14$ for the states with negative and positive parities, respectively, and took the values of n_ρ from zero to 70 for each of the channels. The total number of basis functions used in calculations exceeded 3000. The solution of the problem is somewhat simplified by the fact that the binary α-α subsystem has only even momenta of the relative motion of clusters due to the symmetry.

The choice of the Minnesota potential as a nucleon-nucleon one is not accident. This potential was most frequently used in microscopic calculations of the properties of light atomic nuclei and, in particular, ^{9}Be and ^{9}B [12, 15, 17]. This circumstance facilitates the comparison of our results with those obtained in the other theoretical works. We note that the exchange parameter u of the potential in the mentioned works was chosen to be 0.94 in order to reproduce the properties of the binary subsystems α+α and α+nucleon most properly. However, such a choice of the parameter u implies that nucleus ^{9}Be becomes overbound, and a bound state appears in nucleus ^{9}B.

Prior to the calculation of the three-cluster systems, we studied how strongly the choice of the parameter u of the Minnesota potential affects the characteristics of the resonance states of two-cluster subsystems. In Table 1, we show the energies and the widths of resonances of nuclei ^{8}Be, ^{5}He, and ^{5}Li calculated with $u = 0.928$ and $u = 0.94$.

The results of calculations of the spectra of nuclei ^{8}Be, ^{5}He, and ^{5}Li performed by us with $u = 0.94$ are in good agreement with experimental data. Naturally, the decrease of u to 0.928 somewhat increases the energies of the resonances and their widths, since the odd components of the nucleon-nucleon potential grow, but their values remain reasonable.

In brief, we consider the results obtained for the ground state of nucleus ^{9}Be. It is a bound state, and we can trace easily the convergence of its energy with the use of Fig. 1, as the basis is extended. In this figure, we present the binding energy E versus the total number of basis states N_{fun} used in the calculation. The breaking point on the curve is located at the point, where the basis functions with $L^\pi = 2^-$ are added to the states with $L^\pi = 1^-$. At this point, the energy becomes negative (becomes less than the three-particle threshold), which indicates the importance of the consideration of spin-orbit forces. We recall that this calculation was performed with the maximum value of hypermoment ($K = 13$).

For the analysis of the size of nucleus ^{9}Be, we present the proton, neutron, and mass root-mean-square radii calculated by us: $R_p = 2.27$ Fm, $R_n = 2.46$ Fm, and $R_m = 2.38$ Fm. As would be expected, the radius of the neutron cloud is larger than that of the proton one. We can compare the proton radius with the experimental values. For example, the recent work [28] gives $R_p = 2.519(12)$ Fm, which is close to the result in [17] and can indicate the higher clusterization of the nucleus than that in our model. On the whole, the experimental data deviate to the

Table 1. **Comparison of the parameters of the resonance states of two-cluster subsystems calculated with $u = 0.928$ and $u = 0.940$ with experimental data. The energies and the widths of the resonance states are given in MeV**

		AV RGM				Experiment	
		$u = 0.928$		$u = 0.940$			
Nucleus	J^π	E	Γ	E	Γ	E	Γ
^{8}Be	0^+	0.17	7.15×10^{-4}	0.02	1.03×10^{-7}	0.09	5.6×10^{-6}
	2^+	3.09	1.81	2.93	0.51	3.13	0.51
	4^+	12.91	5.63	12.57	5.02	11.5	3.50
^{5}He	$\frac{3}{2}^-$	1.06	1.17	1.00	1.04	0.80	0.65
	$\frac{1}{2}^-$	2.26	8.63	2.24	8.38	2.07	5.57
^{5}Li	$\frac{3}{2}^-$	1.93	2.00	1.86	1.80	1.69	1.23
	$\frac{1}{2}^-$	3.11	10.24	3.10	9.96	3.18	6.60

Table 2. **Parameters of the lowest states of nucleus ^{9}Be. The energy is measured from the $\alpha + \alpha + n$ threshold**

	AV RGM				Experiment [3]	
	First state		Second state			
J^π	E (MeV)	Γ (keV)	E (MeV)	Γ (keV)	E(MeV$\pm$keV)	Γ (keV)
$\frac{3}{2}^-$	–1.56	–	0.85	261.08	–1.57	–
$\frac{1}{2}^+$	0.25	14.63	–	–	0.11 ± 7	217 ± 10
$\frac{5}{2}^-$	0.99	0.54	2.11	448.24	0.85 ± 1.3	0.78 ± 13
$\frac{1}{2}^-$	0.79	142.77	1.68	458.23	1.23 ± 120	1080 ± 110
$\frac{5}{2}^+$	1.48	315.92	2.60	264.30	1.48 ± 9	282 ± 11

larger side from ours not so strongly (see, e.g., [3], where $R_p = 2.3917$ Fm).

To give a more complete information about the structure of the ground-state wave function of nucleus ^{9}Be, we present Fig. 2 showing the weight W_{sh} of the contribution of each oscillator shell to the wave function, which is normalized to 1. The shells are successfully enumerated so that the shell number N_{sh} corresponds to the principal quantum number $N = 2 \times N_{sh}+3$. The plot is cut on the right side at N_{sh}=22, though the calculation involved all functions of 70 oscillator shells. The plot indicates that the wave function is distributed over a rather large number of shells, which is a manifestation of the strong clusterization of the nucleus.

Before the consideration of the resonance states of nuclei ^{9}Be and ^{9}B, we recall that our main tool for the determination of parameters of the resonance states are the eigenphases of scattering. Their behavior is shown by Fig. 3 presenting the dependence of the eigenphases of scattering on the energy for the state $J^\pi = 3/2^-$ of nucleus ^{9}Be. From three curves, only one reveals the resonance behavior, which allows us to obtain, with the use of (10), the resonance parameters. To complete the pattern, we note that the resonance can manifest itself in some cases in at least two eigenphases.

The basic quantitative characteristics of the bound and resonance states of nuclei ^{9}Be and ^{9}B, obtained in our calculations, are presented in Tables 2 and 3 and in Figs. 4 and 5 together with relevant experimental data. In these calculations, we limited ourselves by the excitation energies of at most 5 MeV. From the

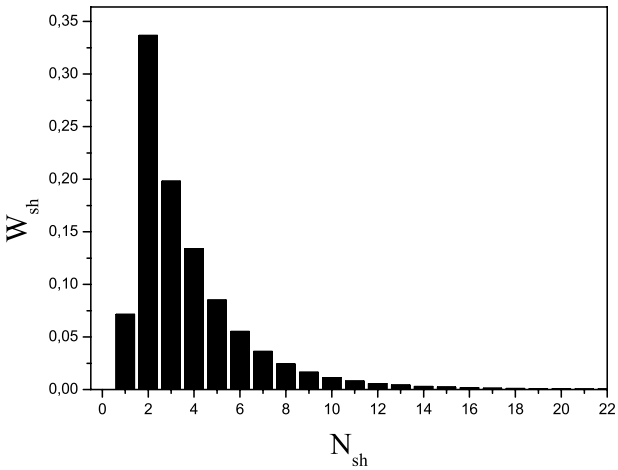

Fig. 2. Contributions of various oscillator shells to the ground state of nucleus ^{9}Be

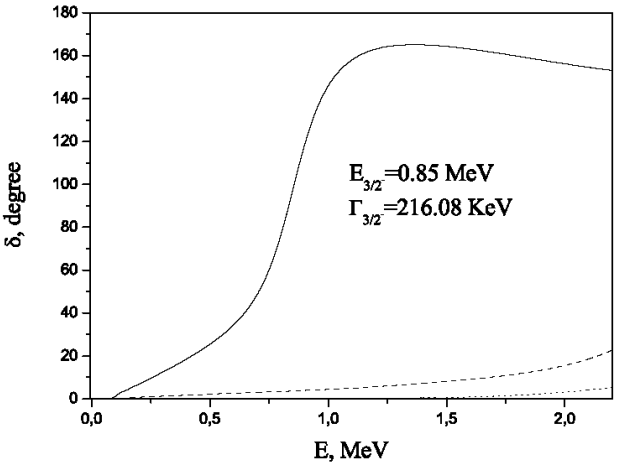

Fig. 3. Eigenphases of scattering for the state J^π=3/2$^-$ of nucleus ^{9}Be

Table 3. **Parameters of the lowest states of nucleus ^{9}B. The energy is measured from the $\alpha + \alpha + n$ threshold**

	AV RGM				Experiment [3]	
	First state		Second state			
J^π	E (MeV)	Γ (keV)	E (MeV)	Γ (keV)	E(MeV±keV)	Γ (keV)
$\frac{3}{2}^-$	0.29	0.39	1.30	460.99	0.28	0.54 ± 21
$\frac{1}{2}^+$	0.59	121.65	–	–	–	–
$\frac{5}{2}^-$	2.60	692.67	2.77	31.48	2.64 ± 5	81 ± 21
$\frac{1}{2}^-$	1.44	185.13	2.83	587.33	3.03 ± 300	3.130 ± 20
$\frac{5}{2}^+$	1.90	459.19	3.77	851.76	3.07 ± 30	550 ± 40

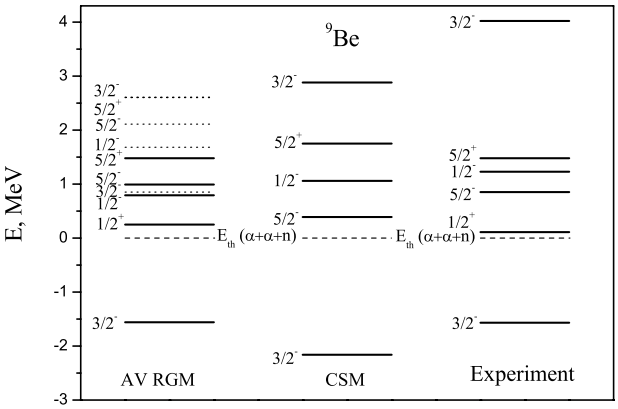

Fig. 4. Calculated and experimental spectrum of ^{9}Be. Calculated spectrum is presented by results of our model (AV RGM) and the Complex Scaling Method (CSM) from Ref. [17]. Experimental data is taken from Ref. [3]

viewpoint of the shell model, these are the energies, at which the states of valent neutron (proton) dominate.

It is seen at once that the region of energies under study includes two and more resonance states, whereas only one state is usually observed in experiments. It is worth noting that we have already met a similar situation, for example, in the calculation of parameters of the 0^+ and 2^+ resonances of nuclei ^{6}He and ^{6}Be. In the reasonable agreement with experiments, we obtained also some resonances with higher energies and large widths [29].

First, such a situation was perceived by us as some drawback of our approach caused by a too high kinematic barrier in the three-particle exit channels. However, the calculations performed with the Complex Scaling Method [30, 31], which is not related to the hyperspherical basis and the form of boundary conditions, indicate also the possibility of the existence of similar resonances.

The spectra of nuclei ^{9}Be and ^{9}B are much richer than those of ^{6}He and ^{6}Be; therefore, the situation turns out, naturally, more complicated. In whole, our model reproduces fairly well the experimental situations for ^{9}Be, if we take "first resonance states" into account. This can be seen in Table 2 and also in Fig. 4, where we display our results, results of the Complex Scalling Method (CSM) from Ref. [17], and experimental data from Ref. [3]. Note that the width of the $1/2^+$-resonance state, obtained in our model, is smaller than its value deduced from experimental data. As is seen in Fig. 4, the first excited state, determined within the CSM, is the $5/2^-$ resonance. However, this resonance in our model lies at a higher energy, as it is observed in experiments. Note that, at this energy, i.e. $E \approx 0.4$ MeV, other methods, used in Ref. [17], predict the existence of the $1/2^+$-resonance state. The difference between the results of our model and the CSM can be ascribed to the different values of the parameter u of the Minnesota potential used in our calculation and in Ref. [17]. This can be also related to properties of the bases, involved in these two calculations.

In the case of ^{9}B, our results almost exactly coincide with the experimental energies of the $3/2^-$ ground state and the $5/2^-$ resonance (see Fig. 5 and Table 3). However, between these two states, our model generates a set of resonance states, which are not observed experimentally. In this energy range, we

display the experimental level the (Fig. 5), which is marked as "$1/2^+$?". Here, we also have the $1/2^+$ resonance state, as well as other states. It is well known that nucleus ^{9}B is a rather complicated object for experimental investigations and has not been studied thoroughly. Thus, we assume that these states can be determined, for instance, in complete kinematic experiments.

It is worth to note that there are two very close resonance states just above the $5/2^-$ resonance in ^{9}B. In experiment, they are the $1/2^-$ and $5/2^+$ states, while, in our calculations, we have the $5/2^-$ and $1/2^-$ states. Comparing results for the mirror nuclei ^{9}Be and ^{9}B calculated within our model and the Complex Scaling Method, we can evaluate the role of the Coulomb interaction. One notices that the Coulomb interaction shifts more strongly the excited states in ^{9}B with respect to those of ^{9}Be in the CSM than in our model. In addition, this interaction in the CSM does not change the order of excited states.

Among the states of nucleus ^{9}B, the $1/2^+$-state is of special interest. As was mentioned above, this state was not included in the spectra in the recent work [3], though its existence was discussed many times in experimental works (see, e.g., [4,32–35] and references therein), where its excitation energy varied from 0.8 to 1.8 MeV, and the width did from 400 to 1300 keV. For this state, we predict a very low excitation energy of about 0.3 MeV and a width of 122 keV, which are less than those in the available theoretical works. For example, $E_x = 1.0$ MeV, $\Gamma = 1.8$ MeV [36]; $E_x = 0.94$ MeV, $\Gamma = 1.64$ MeV [16]; $E_x = 1.3$ MeV, $\Gamma = 2.0$ MeV [37]; and $E_x = 1.2$ MeV, $\Gamma = 1.3$ MeV [12]. In this case, we recall that the analogous state $1/2^+$ in nucleus ^{9}Be obtained by us has a reasonable value of excitation energy, but the width is less than the experimental one.

As was indicated above, the problem under consideration is a many-channel one. It includes the specific channels, which can be classified with the help of the hypermoment K and the partial momenta l_1 and l_2. In this case, we associate the partial momentum l_2 to the binary subsystem $\alpha - \alpha$. The technique of determination of the partial decay widths for such channels was proposed in [38]. Our experience of the calculation of partial widths indicates that the total width is usually composed of contributions of a small number of channels with the minimum values of hypermoment K and with the relevant values of partial

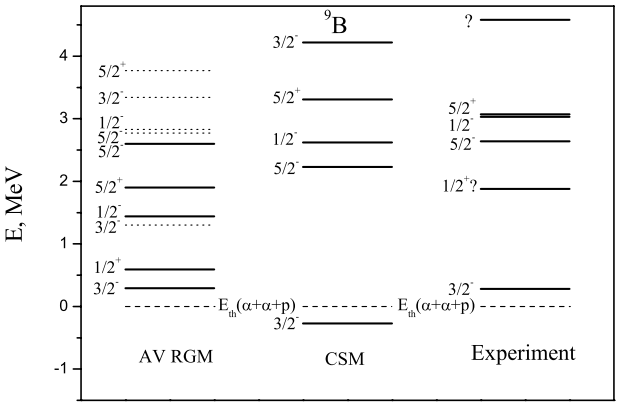

Fig. 5. Calculated and experimental spectra of ^{9}B. Calculated spectrum is presented by results of our model (AV RGM) and the Complex Scaling Method (CSM) from Ref. [17]. Experimental data are taken from [3]

angular momenta. Probably, this is caused by a fast increase in the height and the width of the kinematic barrier with K for three-particle-decay channels. For the comparatively narrow resonances, with which we deal in the present work, the width is determined by only a single channel. Indeed, 99% of the total width of the state of nucleus ^{9}Be with $E_{3/2^-} = 0.85$ MeV, $\Gamma_{3/2^-} = 261.08$ keV are determined by the channel with $K = 1$, $l_1 = 1$, $l_2 = 0$, and the total width of the state of the same nucleus with $E_{1/2^+} = 0.25$ MeV, $\Gamma_{1/2^+} = 14.63$ keV is completely determined by the channel with $K = 0$, $l_1 = 0$, $l_2 = 0$.

4. Conclusions

Within the three-cluster microscopic model, we have studied the spectra of the low-lying states of nuclei ^{9}Be and ^{9}B. To classify the channels of the three-cluster continuum, we used the basis of hyperspherical functions. In the numerical calculations of the bound and resonance states of these nuclei, we involve a large number of hyperspherical and hyperradial states to achieve the convergence of results with suitable accuracy. It is shown that the theory reproduces satisfactorily the experimental structure of excited states of nuclei ^{9}Be and ^{9}B. It turns out that our theoretical spectra contain more states than the available experimental ones. The dominating channels of decay of three-cluster resonances are revealed.

1. S.E.R. Woosley and R.I. Hoffman, Astrophys. J. **395**, 202 (1992).

2. B.S. Meyer, G.J. Mathews, W.M. Howard *et al.*, Astrophys. J. **399** 656 (1992).
3. D.R. Tilley, J.H. Kelley, J.L. Godwin *et al.*, Nucl. Phys. A **745**, 155 (2004).
4. M.A. Tiede, N.R. Robson, D. Caussyn *et al.*, Phys. Rev. C **52**, 1315 (1995).
5. K. Shoda and T. Tanaka, Phys. Rev. C **59**, 239 (1999).
6. H. Akimune, M. Fujimura, M. Fujiwara *et al.*, Phys. Rev. C **64**, 041305(R) (2001).
7. H. Utsunomiya, Y. Yonezawa, H. Akimune *et al.*, Phys. Rev. C **63**, 018801 (2001).
8. B.R. Fulton, R.L. Cowin, R.J. Woolliscroft *et al.*, Phys. Rev. C **70**, 047602 (2004).
9. Y. Prezado, M.J.G. Borge, Aa. Diget *et al.*, Phys. Lett. B **618**, 43 (2005).
10. P. Papka, T.A.D. Brown, B.R. Fulton *et al.*, Phys. Rev. C **75**, 045803 (2007).
11. O. Burda, P. Von Neumann-Cosel, A. Richter *et al.*, Phys. Rev. C **82**, 015808 (2010).
12. P. Descouvemont, Phys. Rev. C **39**, 1557 (1989).
13. V.T. Voronchev, V.I. Kukulin, V.N. Pomerantsev, and G.G. Ryzhikh, Few-Body Syst. **18**, 191 (1995).
14. F.C. Barker, Phys. Rev. C **53**, 2539 (1996).
15. K. Arai, Y. Ogawa, Y. Suzuki, and K. Varga, Phys. Rev. C **54**, 132 (1996).
16. V.D. Efros and J.M. Bang, Eur. Phys. J. A **4**, 33 (1999).
17. K. Arai, P. Descouvemont, D. Baye, and W.N. Catford, Phys. Rev. C **68**, 014310 (2003).
18. K. Arai, Nucl. Phys. A **738**, 342 (2004).
19. L.V. Grigorenko and M.V. Zhukov, Phys. Rev. C **72**, 015803 (2005).
20. M. Theeten, D. Baye, and P. Descouvemont, Phys. Rev. C **74**, 044304 (2006).
21. I. Filikhin, V.M. Suslov, and B. Vlahovic, Few-Body Syst. **50**, 255 (2010).
22. V.S. Vasilevsky, A.V. Nesterov, F. Arickx, and J. Broeckhove, Phys. Rev. C **61**, 034606 (2001).
23. A.V. Nesterov, F. Arickx, J. Broeckhove, and V.S. Vasilevsky, Phys. Part. Nucl. **41**, 716 (2010).
24. G.F. Filippov, I.P. Okhrimenko, Yad. Fiz. **32**, 932 (1980).
25. V.S. Vasilevsky and F. Arickx, Phys. Rev. A **55**, 265 (1997).
26. D.R. Thompson, M. Lemere, and Y.C. Tang, Nucl. Phys. A **286**, 53 (1977).
27. I. Reichstein and Y.C. Tang, Nucl. Phys. A **158**, 529 (1970).
28. W. Nörtershäuser, D. Tiedemann, M. Žáková *et al.*, Phys. Rev. Lett. **102**, 062503 (2009).
29. V.S. Vasilevsky, A.V. Nesterov, F. Arickx, and J. Broeckhove, Phys. Rev. C **63**, 034607 (2001).
30. S. Aoyama, S. Mukai, K. Kato *et al.*, Prog. Theor. Phys. **93**, 99 (1995).
31. S. Aoyama, S. Mukai, K. Kato *et al.*, Prog. Theor. Phys. **94**, 343 (1995).
32. M. Burlein, H.T. Fortune, P.H. Kutt *et al.*, Phys. Rev. C **38**, 2078 (1988).
33. N. Arena, Seb. Cavallaro, G. Fazio *et al.*, EPL **5**, 517 (1988).
34. M.A. Tiede, K.W. Kemper, N.R. Fletcher *et al.*, Phys. Rev. C **52**, 1315 (1995).
35. L. Buchmann, E. Gete, J.C. Chow *et al.*, Phys. Rev. C **63**, 034303 (2001).
36. R. Sherr and H.T. Fortune, Phys. Rev. C **70**, 054312 (2004).
37. N. Tanaka, Y. Suzuki, K. Varga, and R.G. Lovas, Phys. Rev. C **59**, 1391 (1999).
38. V.S. Vasilevsky, F. Arickx, J. Broeckhove, P. Helinckx, and A.V. Nesterov, J. Phys. G **34**, 1955 (2007).

Received 18.04.13

О.В. Нестеров, В.С. Василевський, Т.П. Коваленко

СПЕКТРИ ЯДЕР ^{9}Be ТА ^{9}B У ТРИКЛАСТЕРНІЙ МІКРОСКОПІЧНІЙ МОДЕЛІ

Р е з ю м е

Із застосуванням кластерного представлення α+α+n(p) в рамках трикластерної мікроскопічної моделі – алгебраїчної версії метода резонуючих груп – розглянуто спектри низьколежачих станів дзеркальних ядер ^{9}Be та ^{9}B, що належать області енергій з енергією збудження до 5 МеВ. Отримані теоретичні результати порівняно з існуючими експериментальними даними.

А.В. Нестеров, В.С. Василевский, Т.П. Коваленко

СПЕКТРЫ ЯДЕР ^{9}Be И ^{9}B В ТРЕХКЛАСТЕРНОЙ МИКРОСКОПИЧЕСКОЙ МОДЕЛИ

Р е з ю м е

С использованием кластерного представления α+α+n(p) в рамках трехкластерной микроскопической модели – алгебраической версии метода резонирующих групп – рассмотрены спектры низколежащих состояний зеркальных ядер ^{9}Be и ^{9}B лежащих в области энергий возбуждения до 5 МэВ. Проводится сравнение полученных теоретических результатов с имеющимися к настоящему времени экспериментальными данными.